Vision-Aided Measurement Level Integration of Multiple GPS Receivers for UAVs

Akshay Shetty and Grace Xingxin Gao
University of Illinois at Urbana-Champaign

BIOGRAPHY

Akshay Shetty is a graduate student in the Department of Aerospace Engineering, University of Illinois at Urbana-Champaign. He received his B.Tech. in Aerospace Engineering from Indian Institute of Technology Bombay, India in 2014. On graduation, he was awarded the Institute Silver Medal. His research interests include navigation and control of aerospace systems.

Grace Xingxin Gao is an assistant professor in the Aerospace Engineering Department at University of Illinois at Urbana-Champaign. She received her B.S. degree in Mechanical Engineering in 2001 and her M.S. degree in Electrical Engineering in 2003, both at Tsinghua University, China. She obtained her Ph.D. degree in Electrical Engineering at Stanford University in 2008. Before joining Illinois at Urbana-Champaign as an assistant professor in 2012, Prof. Gao was a research associate at Stanford University. Prof. Gao has won a number of awards, including RTCA William E. Jackson Award, Institute of Navigation Early Achievement Award, 50 GNSS Leaders to Watch by GPS World Magazine, and multiple best presentation awards at ION GNSS conferences.

ABSTRACT

Robust and reliable navigation of Unmanned Aerial Vehicles (UAVs) is an upcoming and promising field of research. In this paper we describe tightly-coupled initialization procedure using a monocular camera to resolve the GPS carrier phase integer ambiguities. This helps us obtain heading estimates during flight, using the GPS receivers. Further, we describe a sensor fusion structure which uses the measurements from multiple GPS receivers and multiple sensors on-board a UAV. We implement an unscented Kalman filter (UKF) to fuse information from the GPS receivers, the monocular camera, the inertial measurement unit (IMU) and the motor tachometers. In the filter we use pseudoranges and carrier phases from the GPS receivers, as opposed to directly using the position updates. Experiments were conducted outdoors with an Ascending Technologies Firefly hexacopter. We validate the integer ambiguity resolution by our tightly coupled initialization, and the robust sensor fusion structure.

INTRODUCTION

Unmanned Aerial Vehicles (UAVs) have emerging applications such as mapping, surveillance, precision agriculture, delivering packages and television coverage of events. However, the primary concerns of safety continue to delay the surge of UAVs for commercial applications. While using a small flying robot has its own advantages, it is important to ensure reliable navigation which translates to reliable estimation and control algorithms on the UAV.

The quality of estimation determines the safety and maneuverability of the UAV. Thus it is common practice to rely on multiple sensors, opposed to measurements from just a single sensor. UAVs can be equipped with several onboard sensors like the inertial measurement units (IMU), global positioning system (GPS) receivers, cameras, pressure sensors, depth sensors, etc. This redundancy in measurements protects the UAV during events of having unavailable or corrupted sensor measurements. However due to constraints on the payload an UAV can carry, it is important to efficiently combine the available sensors. Different algorithms including particle filters, Kalman filters and its variations are commonly implemented for sensor fusion.

One of the major challenges in combining measurements from multiple sensors is to handle the computational workload and provide estimates in real-time. Various methods have been investigated for sensor-fusion in the field of UAVs, with the most common being the Kalman filters [1], [2]. The extended Kalman filter (EKF) can handle some non-linear measurements and is computationally lighter relative to some other Kalman filter variations in [3]. On the other hand, the unscented Kalman filter (UKF) is computationally heavier but is able to capture higher order non-linearities.

There are several non-linear estimation methods proposed for UAV navigation. Some of them include using a non-linear complementary filter [4] to estimate the attitude of

a UAV to aid vertical take-off and landing and Sigma point Kalman filters [5] for integrating GPS with an IMU and an altimeter. [6] presents a detailed analysis of the unscented Kalman filter for an UAV GPS-IMU sensor fusion. However, in most of these works the position solution from the GPS receivers is directly used to update the states of the filter. The works of [7] and [8] focus on a more tightly coupled GPS-inertial structure using unscented Kalman and Particle filters. While the position of the UAV might be our primary concern, it might not always be possible for the receiver to provide a position update. During the motion of the UAV, there might be situations where the receiver loses track of satellites due to fast maneuvers or obstructions. In cases where the number of tracked satellites drops below four, the GPS receiver will not be able to estimate the position of the UAV and thus will not provide any correction to sensor fusion model. However, the receiver still tracks some satellites and generates measurements which are unused in the above case. In our previous work [9] we had outlined the advantages of using the measurements as corrections in the Kalman filter, as opposed to directly using the position.

Different techniques of incorporating vision for navigation have been implemented previously. In [10] a charge coupled device (CCD) video camera is used along with a laser rangefinder to estimate the movements of the UAV. Cameras can also be used in a stereo setup which helps in recovering 3D information from the scene. [11] presents combination of a forward-facing stereo setup and sidefacing cameras using optical flow. Experiments conducted on a ground-based tractor and an UAV in urban canyons showed the advantages of combining both the methods.

Recently there has been an increasing focus on algorithms for estimating the movements of monocular cameras. State of-art methods like [12], [13] and [14] provide scaled 5-DOF pose measurements at frequencies suitable for real-time applications. Large-scale direct SLAM [13] creates and stores a 3D map of its environment, which increases the load as the number of points increases. Parallel tracking and mapping (PTAM) [12] and semi-direct visual odometry (SVO) [14] track limited number of points across frames, thus making them computationally lighter. Of these two methods, SVO has been demonstrated to work better than PTAM on scenes with high-frequency texture like tiles and grass. This is advantageous for flight in new unknown areas which might not have many visible features available for the camera. However, the ground plane estimation in PTAM is better than that in SVO, thus providing more reliable attitude updates to the filter. While flying outdoors, bright lighting conditions help us to operate at higher camera frame rates of more than 70 frames per second. This enables PTAM to function properly even during scenarios with a small number of features. Hence for our application we use the PTAM algorithm to provide us with the 5-DOF pose measurements. Figure 1 shows a snapshot of the PTAM algorithm.

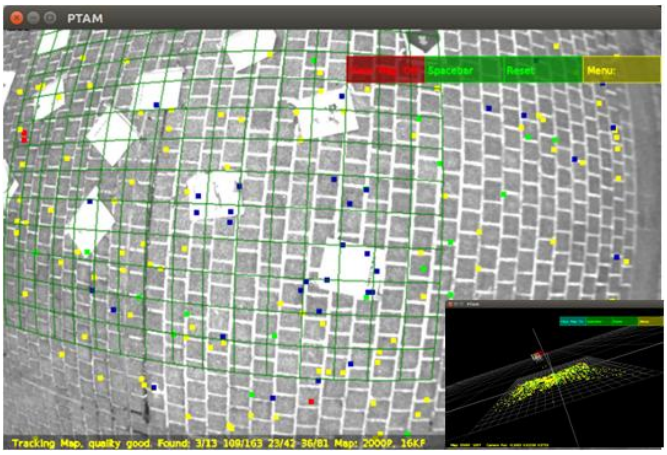

Figure. 1. Parallel Tracking and Mapping (PTAM). Algorithm tracks features across images and re-projects them on a point cloud to estimate the cameras pose (bottom right).

In this paper we continue working on the measurement-level integration [9], incorporating the carrier phase measurements into the structure. However, these measurements contain integer ambiguities and there are various methods presented in literature to resolve them. Previous works in [15-19] use information only from the GPS receivers and/or are validated for long baselines. In our work, we present an initialization procedure using information from a camera to resolve the integer ambiguities for short baselines on UAVs.

We use multiple low-cost and light-weight GPS receivers on a UAV, along with information from a camera, IMU and the motors. Figure 2 shows the layout of the setup and labels the different components.

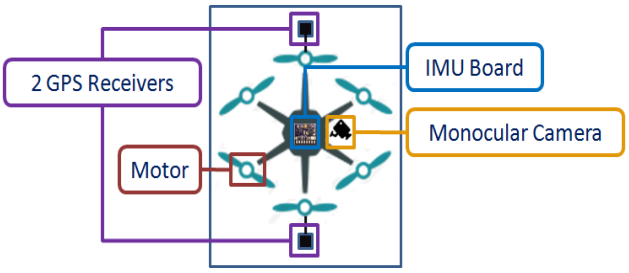

Figure 2. Components layout. Information sources for navigation: 2 GPS receivers, Monocular camera, IMU board and motors.

In the following sections, we begin with discussing the tightly-coupled initialization approach we have taken. We then proceed to describe the unscented Kalman filter (UKF), where we show the prediction and measurement

models being used within the filter. This is followed by a section on our experimental setup and how the different hardware components interact with each other. Finally we discuss the results and present our conclusions.

TIGHTLY-COUPLED INITIALIZATION

In our initialization procedure, we estimate the integer ambiguities related to the carrier phase measurements using attitude information from the vision algorithm. Once the integer ambiguities are estimated, they are used during flight to estimate the baseline, and hence the heading. Figure 3 gives an overview of the initialization process.

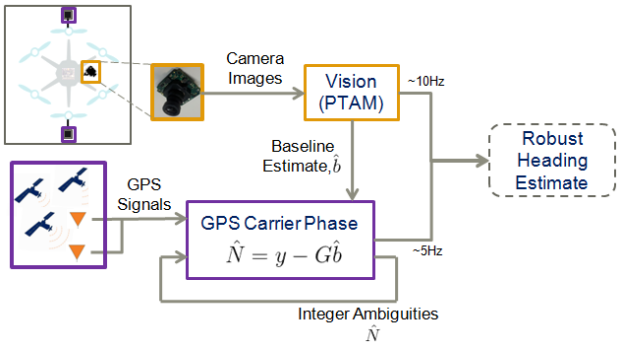

Figure. 3. Tightly-coupled initialization procedure to resolve carrier phase integer ambiguities. Once the ambiguities are resolved we obtain heading information from the GPS receivers, in addition to the vision algorithm.

We perform our initialization process before beginning the flight. The carrier phase measurements for the GPS receivers from the k^{th} satellite can be represented by the following equation:

$$\phi_u^{(k)} = \lambda^{-1}\left[r_u^{(k)} - I_u^{(k)} + T_u^{(k)}\right] + f\left(\delta t_u - \delta t^{(k)}\right) + N_u^{(k)} + \epsilon_{\phi,u}^{(k)} \quad (1)$$

$\phi_u^{(k)}$: carrier phase between receiver and k^{th} satellite
λ, f: carrier wavelength and frequency
$r_u^{(k)}$: true range between receiver and k^{th} satellite
$I_u^{(k)}, T_u^{(k)}$: ionospheric and tropospheric range errors
$\delta t_u, \delta t^{(k)}$: receiver and satellite clock biases
$N_u^{(k)}$: integer ambiguity in the carrier phase
$\epsilon_{\phi,u}^{(k)}$: measurement noise

We use between-receiver, between-satellite double-difference measurements, called *double differences*. For instance, the double difference between k^{th} and l^{th} satellites, and between 1^{st} and 2^{nd} receivers can be shown as:

$$\phi_{12}^{(kl)} = \lambda^{-1} r_{ur}^{(kl)} + N_{12}^{kl} + \epsilon_{\phi,12}^{(kl)} \quad (2)$$

In this equation, we have rid ourselves from the nuisance parameters, except for the integer ambiguities. To solve for these ambiguities, we make use of all the available double differences. After applying some simple geometric constraints, we can obtain the following equation:

$$\boldsymbol{y} = \boldsymbol{G}.\boldsymbol{b} + \boldsymbol{N} + \epsilon_{\phi} \quad (3)$$

$\boldsymbol{y}$: matrix containing double differences
$\boldsymbol{G}$: observation matrix for receivers-satellites geometry
$\boldsymbol{b}$: baseline vector between the two receivers
$\boldsymbol{N}$: double difference integer ambiguities
ϵ_{ϕ}: double difference noise

A detailed deduction of Eq. 3 from Eq. 2 can be found in [20]. Thus, the goal of the initialization procedure is to estimate the double difference integer ambiguities, $\widehat{\boldsymbol{N}}$:

$$\widehat{\boldsymbol{N}} = \boldsymbol{y} - \boldsymbol{G}.\widehat{\boldsymbol{b}} \quad (4)$$

For every measurement epoch, we create the $\boldsymbol{y}$ matrix with the double differences. $\boldsymbol{G}$ can be created once we have the satellite and the receiver position estimates in the earth-centered earth-fixed (ECEF) co-ordinate frame. This information is obtained from the ephemeris. Finally, we need to determine the baseline vector, $\widehat{\boldsymbol{b}}$ between the two receivers in the ECEF frame. To obtain this, we use attitude measurements from the vision algorithm, PTAM. These measurements help us rotate the fixed baseline vector in the body frame to the local navigation frame, East-North-Up (ENU). We then use the initial latitude-longitude information to rotate the baseline to the ECEF frame. Thus, with the right-hand side of Eq. 4 ready, we proceed to estimate the integer ambiguities.

Once we obtain good estimates, we use these integers for estimating heading during flight.

SENSOR FUSION: Unscented Kalman Filter

The unscented Kalman filter is a variation of the Kalman filter designed to handle cases when the state transition and observation models are non-linear. It uses a deterministic sampling technique known as the unscented transform to pick a minimal set of sigma points around the mean. These sigma points are then propagated through the non-linear functions, from which the mean and covariance of the estimate are then recovered. As a result of these transforms, the filter more accurately captures the true mean and covariance. Further, this technique removes the requirement to explicitly calculate Jacobians which would have been a tedious task for our measurement models. In Figure 4, we show the basic

steps involved in the UKF: the time update and the measurement update.

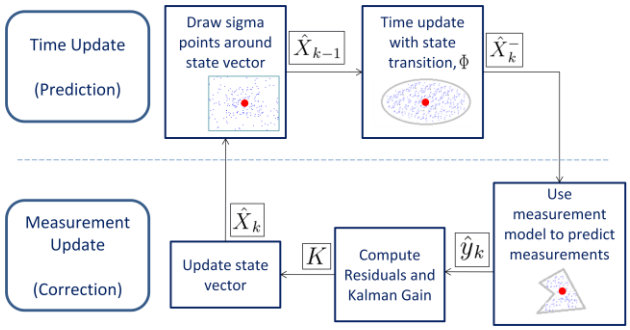

Figure. 4. The unscented Kalman filter (UKF). Consists of the Time update and Measurement update steps. Time update: we use the state transition matrix Φ (Eq. 5) to propagate the states. Measurement update: we use the measurement model to predict measurements, compute the Kalman gain and update the states.

For our sensor fusion we try to make use of all the measurements available from the different sources. The state vector X, used in the filter consists of 25 states, shown in Figure 5.

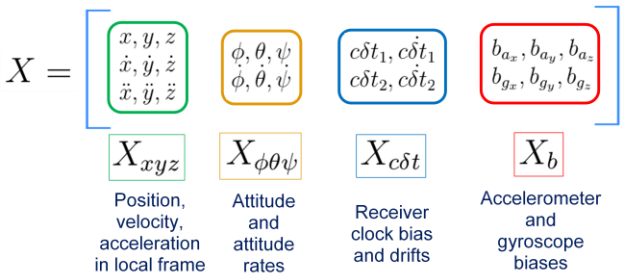

Fig. 5. State vector in the UKF.

The UKF, like any other Kalman filter, consists of two important steps: Prediction and Correction.

A. Prediction Step

The state vector consists of four independent blocks: the position states, the attitude states, the receiver clock bias states and the accelerometer/gyroscope bias states. For the position states we use a constant acceleration model to predict the states at the next time instant, while for the rest we use a forward Euler integration method.

The combined state transition matrix looks as follows:

$$\Phi = \begin{bmatrix} \Phi_{xyz} & 0 & 0 & 0 \\ 0 & \Phi_{\phi\theta\psi} & 0 & 0 \\ 0 & 0 & \Phi_{c\delta t} & 0 \\ 0 & 0 & 0 & \Phi_b \end{bmatrix} \quad (5)$$

The position states depend on the previous positions, velocities and accelerations and are predicted using the following state transition matrix:

$$\Phi_{\text{xyz}} = \begin{bmatrix} 1 & 0 & 0 & \Delta t & 0 & 0 & \frac{\Delta t^2}{2} & 0 & 0 \\ 0 & 1 & 0 & 0 & \Delta t & 0 & 0 & \frac{\Delta t^2}{2} & 0 \\ 0 & 0 & 1 & 0 & 0 & \Delta t & 0 & 0 & \frac{\Delta t^2}{2} \\ 0 & 0 & 0 & 1 & 0 & 0 & \Delta t & 0 & 0 \\ 0 & 0 & 0 & 0 & 1 & 0 & 0 & \Delta t & 0 \\ 0 & 0 & 0 & 0 & 0 & 1 & 0 & 0 & \Delta t \\ 0 & 0 & 0 & 0 & 0 & 0 & 1 & 0 & 0 \\ 0 & 0 & 0 & 0 & 0 & 0 & 0 & 1 & 0 \\ 0 & 0 & 0 & 0 & 0 & 0 & 0 & 0 & 1 \end{bmatrix} \quad (6)$$

The following state transition matrices are used for the other blocks of the state vector:

$$\Phi_{\phi\theta\psi} = \begin{bmatrix} 1 & 0 & 0 & \Delta t & 0 & 0 \\ 0 & 1 & 0 & 0 & \Delta t & 0 \\ 0 & 0 & 1 & 0 & 0 & \Delta t \\ 0 & 0 & 0 & 1 & 0 & 0 \\ 0 & 0 & 0 & 0 & 1 & 0 \\ 0 & 0 & 0 & 0 & 0 & 1 \end{bmatrix} \quad (7)$$

$$\Phi_{c\delta t} = \begin{bmatrix} 1 & 0 & \Delta t & 0 \\ 0 & 1 & 0 & \Delta t \\ 0 & 0 & 1 & 0 \\ 0 & 0 & 0 & 1 \end{bmatrix} \quad (8)$$

$$\Phi_{\text{b}} = I_{6x6} \quad (9)$$

With the prediction model defined, we now discuss the correction step.

B. Correction Step

The different sources of correction for the UKF include: GPS receivers, vision algorithm, IMU board and motor tachometers. From the GPS receivers, we use two kinds of measurements: pseudoranges and carrier phases. The pseudoranges can be related to the states as:

$$\rho_1^k = \sqrt{(x_1 - x_s)^2 + (y_1 - y_s)^2 + (z_1 - z_s)^2} + c\delta t_1 \quad (10)$$

ρ_1^k: pseudorange from k^{th} satellite to receiver corrected for satellite clock bias and atmospheric errors
$(x_s, y_s, z_s)^k$: ECEF position of k^{th} satellite
(x_1, y_1, z_1): ECEF position of receiver
$c\delta t_1$: receiver clock bias

The ECEF position of the receiver is obtained using the first the states of the state vector along with the initial latitude-longitude. The carrier phase measurements from the receivers are used to calculate the heading of the UAV, which affects the yaw state. This is obtained by re-arranging Eq. 4.

$$\hat{\boldsymbol{b}} = \boldsymbol{G}^{-1}(\boldsymbol{y} - \hat{\boldsymbol{N}}) \tag{11}$$

This baseline is then rotated from the ECEF frame to the ENU frame using the initial latitude-longitude. Finally, we estimate the heading angle looking at the orientation of the baseline in this ENU frame.

The second source of measurements, coming from the vision algorithm (PTAM) affects the position and the attitude states. After quickly setting up the scale for PTAM, we start receiving updates for the camera position and attitude. However, when the algorithm loses tracking of the features it is not able to estimate the position and attitude.

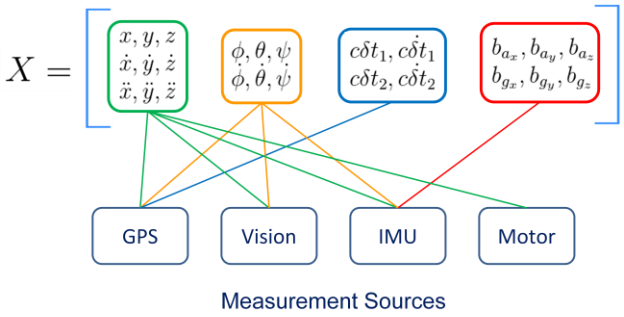

Figure. 6. Correction model block diagram. The four measurement sources affect different states in the Measurement update step of the UKF.

The next source of correction is from the IMU board which consists of 3 axes accelerometers, gyroscopes and magnetometers. The accelerations and the angular velocities are in the body frame of the UAV and are rotated to the local navigation frame using the attitude states. Further the magnetometers estimate the attitude in the local frame. And finally, we also use the motor speed information to estimate the individual motor forces and thus the total thrust along the body axes. This is also transformed into the local frame before being used in the filter. Figure 6 summarizes the states each measurement source affects via the UKF.

EXPERIMENTAL SETUP

To implement our approach, we use the Firefly hexacopter manufactured by Ascending Technologies shown in Fig. 7. The Firefly offers plenty of space and various interfaces for individual components and payloads. This top quality and safe aerial robot is a highly reliable platform for research purposes. For our experiment, we need to record messages from two u-blox receivers simultaneously. In order to log these messages

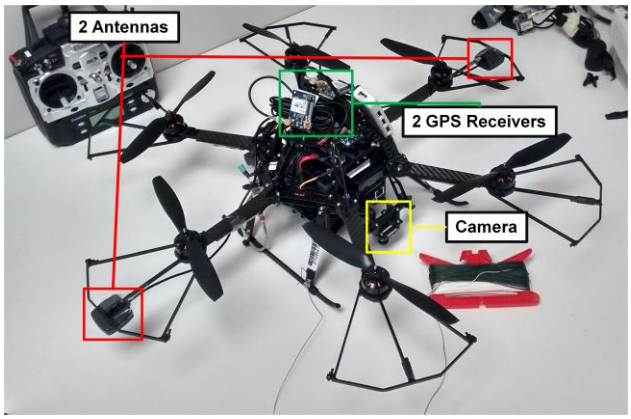

Figure. 7. Ascending Technologies Firefly hexacopter setup used for flight experiments. Two GPS antennas are mounted on opposite arms along with a downward facing camera.

we use an onboard computer, the AscTec Mastermind. The AscTec Mastermind, preinstalled with a Linux OS, has a high performing 3rd Generation Intel® Core™ i7 processor. Further, it has multiple USB ports which allow us to connect the u-blox receivers, along with a camera. We use a MatrixVision camera to record the images and then apply the Parallel Tracking and Mapping (PTAM) method.

Figure 8 shows how the different hardware components in our setup are connected to each other. The GPS receivers and the camera along with the microcontroller on the

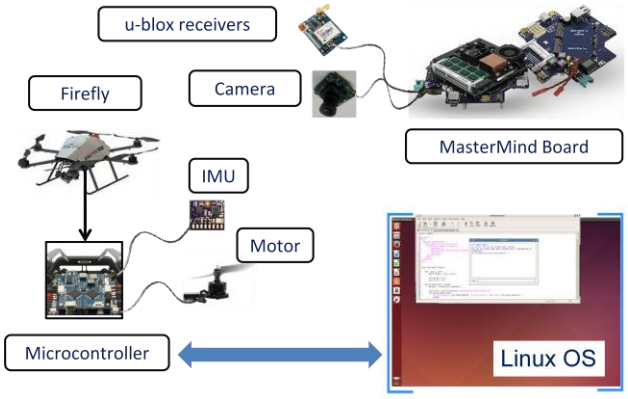

Figure. 8. Hardware components used for collecting flight data. The Mastermind with the Linux OS records all the incoming information used later on for post-processing.

Firefly are connected to the Mastermind. The microcontroller sends information from the IMU board and the motor, over to the Mastermind which records all the messages and images to be used for post-processing.

RESULTS

We first validate the initialization step, where we yaw the Firefly at different angles and record the GPS carrier phase measurements and the vision algorithm (PTAM) attitude estimates. Figure 9 shows the results obtained by using Eq. 4. After some time we are able to settle at integer values. Once the integer ambiguities are estimated, they are stored and used later on to estimate the heading. Eq. 11 is used to estimate the heading using the GPS carrier phase measurements and the integer ambiguities. In Figure 10 we compare the heading estimate obtained using Eq. 11 with the heading estimate obtained using the vision algorithm (PTAM).

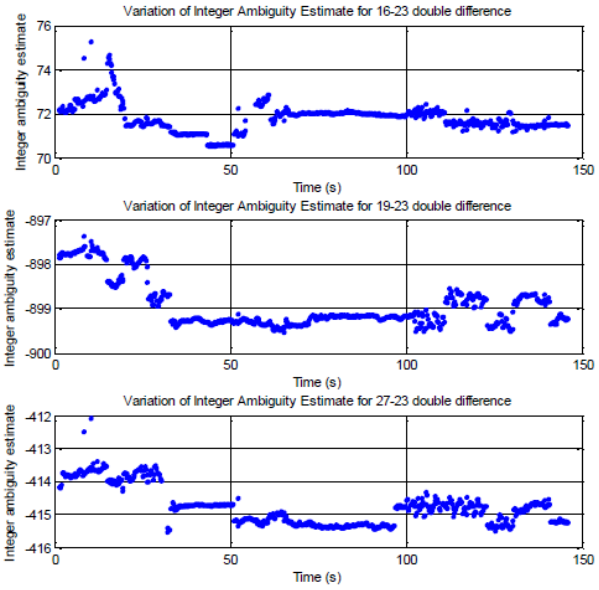

Figure 9. Double difference integer ambiguity estimates over time for 3 available satellite pairs. The estimates settle near integer values over time.

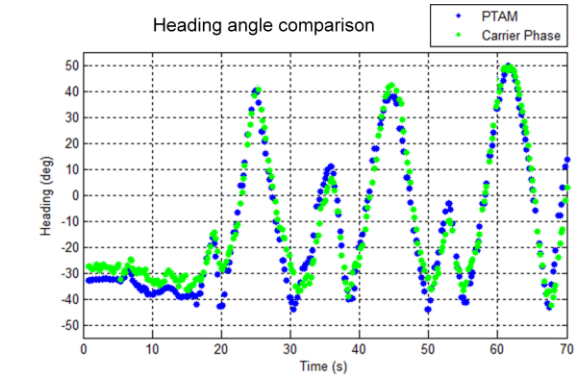

Figure 10. Comparison between the heading estimates obtained from PTAM (blue) and from the GPS carrier phase measurements (green). The heading estimates from the carrier phase measurements accurately match the heading estimates from PTAM.

With heading estimates available from the GPS carrier phases, we began our flight. We followed an approximately rectangular path with the Firefly. We use our sensor fusion structure on the different measurement sources and observe the navigation solution. In Figure 11, we compare the solution obtained in these scenarios. As expected, the navigation solution dependent on just the inertial measurements diverges quickly due to the biases and drifts present in the inertial sensors. The navigation solution dependent on vision follows the true path closely. However, the vision algorithm is not completely reliable as it depends on many factors like the image quality and the frame rate.

The position estimates obtained using just the pseudoranges from the GPS receivers are near the true path but very noisy. Thus, aiding these with the heading information improves the navigation solution, significantly reducing the number of stray points. The overall navigation solution including information from all the sources accurately follows the true path. The solution places higher confidence on the vision algorithm (PTAM) due to its more accurate pose estimates.

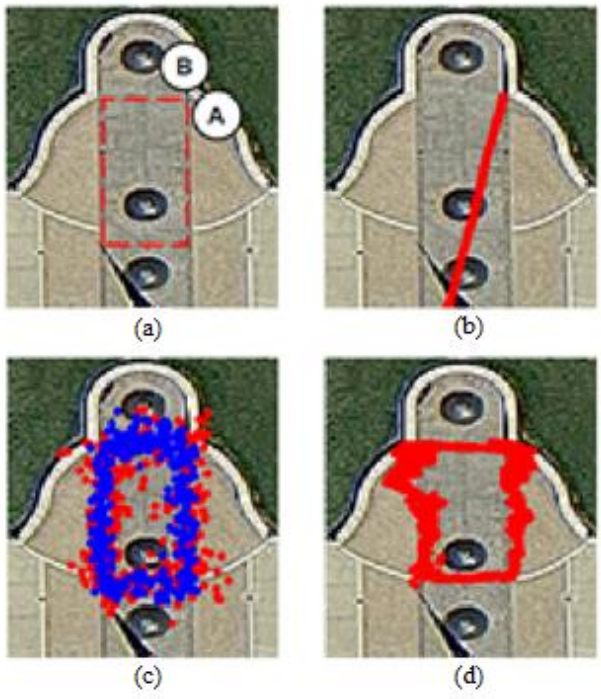

Figure 11. Outdoor flight results. (a) Approximate closed-loop trajectory followed from A to B. Navigation solution obtained using (b) only inertial measurements, (c) only pseudoranges from the GPS receivers (red); pseudoranges and carrier phases from the GPS receivers (blue), (d) 2 GPS receivers, vision (PTAM), IMU and motors for complete navigation solution from the robust sensor fusion. The navigation solution is more accurate after including the heading information from the GPS carrier phase measurements.

CONCLUSIONS

In this paper, we proposed a tightly-coupled initialization procedure for the GPS carrier phase measurements, followed by a robust sensor fusion dependent on multiple GPS receivers and multiple sensors. In the initialization we used attitude estimates from our vision algorithm to estimate the double difference carrier phase integer ambiguities. We then used these integer estimates to obtain a redundant heading estimate and incorporated it in our sensor fusion. Flight tests were conducted outdoors, with two u-blox receivers mounted on a Firefly hexacopter. We were able to validate resolution of the integer ambiguities, along with the heading estimates obtained from the carrier phase measurements. Finally, we could observe improved accuracy in the navigation solution of our vision aided sensor fusion structure.

REFERENCES

[1] J. N. Gross , Y. Gu , M. B. Rhudy , S. Gururajan and M. R. Napolitano "Flight-test evaluation of sensor fusion algorithms for attitude estimation", IEEE Trans. Aerosp. Electron. Syst., vol. 48, pp.2128 -2139 2012.

[2] Jan W., M. Oliver, S. Christian and F. Gert, "An integrated GPS/MEMS-IMU navigation system for an autonomous helicopter", Aerospace Science and Technology 2006, 10: 527-533.

[3] J.J. LaViola, Jr. "A Comparison of Unscented and Extended Kalman Filtering for Estimating Quaternion Motion," Proc. Am. Control Conf., June 2003, vol. 3, pp. 2435-2440.

[4] N. Metni , J.-M. Pflimlin , T. Hamel and P. Soueeres "Attitude and gyro bias estimation for a VTOL UAV", Control Eng. Practice 2006, vol. 14, no. 12, pp.1511-1520.

[5] R. van der Merwe, E.A. Wan and S. Julier, "Sigma-Point Kalman Filters Nonlinear Estimation and Sensor Fusion - Applications in Integrated Navigation", Proc. AIAA Guidance Navigation and Controls Conf., Mar. 2004.

[6] M. Rhudy, Y. Gu, J. Gross, and M. R. Napolitano, "Evaluation of matrix square root operations for UKF within a UAV GPS/INS sensor fusion application", International Journal of Navigation and Observation, vol. 2011, 2012.

[7] J. Zhou, Y. Yang, J. Zhang, E. Edwan, O. Loffeld, and S. Knedlik, "Tightly-coupled INS/GPS using Quaternion-based Unscented Kalman filter", in AIAA Guidance, Navigation and Control, Portland, Oregon, 2011.

[8] A. Rabbou and A. El-Rabbany "Tightly Coupled Integration of GPS Precise Point Positioning and MEMS-Based Inertial Systems", GPS Solution 2014, 1-9.

[9] A. Shetty and G. X. Gao, "Measurement Level Integrationof Multiple Low-Cost GPS Receivers for UAVs," Proceedings of the 2015 International Technical Meeting of The Institute of Navigation, Dana Point, California, January 2015, pp. 842-848.

[10] J. Wang, M. Garratt, A. Lambert, J.J. Wang, S. Han and D. Sinclair, "Integration of GPS/INS/Vision Sensors to Navigate Unmanned Aerial Vehicles", International Society for Photogrammetry and Remote Sensing (ISPRS) Congress, 2008.

[11] S. Hrabar , G. S. Sukhatme , P. Corke , K. A. Usher and J. A. Roberts "Combined optic-flow and stereo-based navigation of urban canyons for a UAV", Proc. IEEE/RSJ Int. Conf. IROS 2005, pp.3309-3316.

[12] G. Klein and D. Murray "Parallel tracking and mapping for small AR workspaces", in Proc. Sixth IEEE and ACM International Symposium on Mixed and Augmented Reality (ISMAR' 07), Nara, Japan, November 2007.

[13] J. Engel, T. Schops, and D. Cremers, "LSD-SLAM: Large-scale direct monocular slam", in Computer Vision ECCV 2014. Springer, 2014, pp. 834849.

[14] C. Forster, M. Pizzoli, and D. Scaramuzza, "SVO: Fast semi-direct monocular visual odometry", in Proc. IEEE Int. Conf. Robotics Automation, 2014, pp. 18.

[15] G. Blewitt "Carrier Phase Ambiguity Resolution for the Global Positioning System Applied to Geodetic Baselines up to 2000 km", Journal of Geophysical Research 1989, Vol. 94, No. B8, pp. 10.187-10.203.

[16] P.J. de Jonge and C.C.J.M. Tiberius "The LAMBDA method for integer ambiguity estimation: implementation aspects", LGR-series 1996, no. 12, Delft Geodetic Computing Centre.

[17] P.J.G. Teunissen, P.J. de Jonge and C.C.J.M. Tiberius "The least-squares ambiguity decorrelation adjustment: its performance on short GPS baselines", submitted to Journal of Geodesy 1995, 16pp.

[18] G. Falco and M. Campo-Cossío Gutiérrez, E. López Serna, F. Zacchello, and S. Bories, "Low-cost Real-time Tightly-coupled GNSS/INS Navigation System Based on Carrier Phase Double Differences for UAV Applications", *Proceedings of the 27th International Technical Meeting of the Satellite Division of The Institute of Navigation (ION GNSS+2014)*, Tampa, Florida USA, pp:841-857.

[19] L. Baroni and H. Koiti, "Analysis of Attitude Determination Methods Using GPS Carrier Phase Measurements", in *Mathematical Problems in Engineering*, Vol. 2012, Hindawi Publishing Corporation, Article ID 596396, p. 10.

[20] P. Misra and P. Enge, "*Global Positioning System: Signals, Measurements, and Performance"*, Revised 2nd ed. Lincoln, MA: Ganga-Jamuna Press, 2012.